Electromagnetic Analysis and Electrical Signature-Based Detection of Rotor Inter-Turn Faults in Salient-Pole Synchronous Machine

Mostafa Valavi, Kari Gjerde Jørstad, and Arne Nysveen

Department of Electrical Power Engineering, Norwegian University of Science and Technology, Trondheim 7034, Norway

In this paper, rotor inter-turn faults in salient-pole synchronous machines are investigated using finite-element (FE) analysis. The machine under study is a 22 MVA 8-pole hydropower generator with fractional-slot windings. Simulated faulty cases include 1, 2, 5, 10, and 20 short-circuited turns (out of 58 turns) in one rotor pole. In the electromagnetic analysis, the effect of faults on airgap flux density and radial forces is studied. Furthermore, the paper investigates on-line detection of inter-turn faults using spectral analysis of stator voltage or current is studied. The amplitude of fault-related harmonics is investigated at various fault severities, as well as at no-load and full-load operations. The paper also discusses the effects of damper bars, influence of parallel circuits in the stator windings, and influence of the pole pair number. In addition, a comparison between fault-related harmonics in the case of dynamic eccentricity and rotor inter-turn faults is presented.

Index Terms—Inter-turn faults, electrical signature analysis, on-line condition monitoring, hydrogenerator, radial forces.

I. INTRODUCTION

ON–LINE condition monitoring of large synchronous machines, including salient-pole hydropower generators, enables the preventive maintenance and improves the reliability of the power generation units. Continuous monitoring of the generator makes it possible to detect the faults at early stages and plan the maintenance actions before they cause major problems and unscheduled shutdowns.

Inter-turn short-circuit faults in the rotor windings of salient-pole machines are caused by insulation failure due to aging, and thermal and mechanical stresses [1, 2]. As a result of short-circuited turns, the total ampere-turn would be reduced in the affected pole and consequently the airgap flux density distribution becomes asymmetric. The consequences, obviously, depends on the severity of the fault. If only a few turns in one pole are short-circuited, the effects are barely noticeable which makes it more difficult to detect at very early stages. The fault, however, might develop; more turns can be short-circuited and the situation may also lead to rotor earth faults that are more serious. In the case of major inter-turn faults, the asymmetry of the airgap field could cause considerable unbalanced magnetic pull (UMP) and vibration problems [3].

During scheduled shutdowns, off-line measurements (e.g. voltage drop test and recurrent surge oscillography method [1]) can be employed for rotor windings inspection and finding the short-circuited turns. A well-known on-line method is to install flux sensors inside the machine to be able to monitor the airgap field [1, 2, 4]. If stator windings consist of parallel circuits, measurement of the circulating current caused by the asymmetry in the airgap field may also be used for on-line fault detection [1, 5]. Vibration analysis may also be capable of detecting the inter-turn rotor faults, by monitoring the fault-related frequency components in the vibration spectrum [1, 6]. Analysis of the leakage flux (using sensors outside the machine) is another on-line method proposed in the literature [6].

This paper investigates the use of electrical signature analysis [7, 8] for on-line detection of rotor inter-turn faults in salient-

TABLE I
SPECIFICATIONS OF SIMULATED HYDROGENERATOR

Power	22 MVA
Speed	750 rpm
Number of slots	126
Number of poles	8
Number of turns per rotor pole	58
Rotor field current (resistive load)	440 A
Number of damper bars per pole	8
Airgap diameter	2017 mm
Machine length	1220 mm
Nominal terminal voltage	7700 V *rms*
Nominal terminal current	1650 A *rms*

pole synchronous machines. In this method, spectral analysis of electrical signals (e.g. current, voltage and power) are employed to detect mechanical (e.g. eccentricity and bearing faults [9]) and electrical faults (e.g. short-circuit in stator or rotor windings [10]) in the electrical machines. Electrical signature analysis is well covered in the literature and has been applied for detection of different faults in various types of electrical machines. However, to the best of the authors' knowledge, the method has not yet been investigated thoroughly for rotor inter-turn fault diagnosis in salient-pole synchronous machines. Recently in [11], the capability of electrical signature analysis for fault detection in a prototype synchronous machine is confirmed experimentally in the case of a relatively severe rotor inter-fault test. The focus of the work in [11] is discrimination between eccentricity and inter-turn faults using electrical signals of all three phases and investigation is based on only one fault-related harmonic.

In this paper, finite element (FE) analysis is employed to study inter-turn faults in rotor windings of a synchronous hydropower generator, taking into account the fault severity (ranging from as few as only 1 to as many as 20 short-circuited turns out of total 58 turns in one pole), effect of damper bars and influence of having parallel circuits in the stator windings. The research work is carried out to examine the effectiveness

of spectral analysis of stator voltage (or current) in order to detect the rotor inter-turn faults in early stages. It is worth mentioning that no similar study has been found in the literature.

The presented method is based on the magnetic asymmetry in the airgap, caused by a reduced ampere-turn in the faulty pole. As will be discussed further in Section II, fault (i.e. short-circuited turns) is simply modeled by a reduction in the ampere-turn of the rotor pole. It should be noted that in practice, a resistance layer with damaged insulation is formed due to the short circuit and current in the shorted turns depends on the value of this resistance. Needless to say that if insulation is damaged but the total ampere-turn of the pole is not sufficiently reduced, the presented method cannot detect the fault. In addition, it is worth noting that the presented method cannot locate the fault in the windings. As an online condition monitoring method which only needs stator voltage or current, it can be effectively used to issue warnings regarding magnetic asymmetry in the machine and potential cause for that, thus helping to schedule maintenance actions. For further investigations and locating the faults, other methods including airgap flux sensors and offline measurements can be employed.

The paper is organized as follows. In Section II, electromagnetic analysis is presented; details of FE modeling and analysis are explained and the effect of rotor faults on flux density and force density distributions is addressed. Section III presents the fault detection method based on the spectral analysis of stator voltage (or current). The effects of damper bars and parallel circuits are investigated in Section IV and V, respectively. Influence of pole pair number is addressed in Section VI. In addition, differentiation between eccentricity and rotor inter-turn faults is discussed in Section VII. Section VIII presents the concluding remarks.

Specifications of the hydrogenerator under investigation are listed in Table I.

II. ELECTROMAGNETIC ANALYSIS

In this section, FE modeling and simulations, flux density distribution and radial forces are discussed, addressing the effects of the inter-turn faults.

A. FE Modeling and Simulations

Time-stepping FE analysis is employed for modeling and simulation of rotor inter-turn faults. Since the simulation results will be used to identify fault-related harmonics, special attention must be paid to the quality of mesh (especially in the airgap), time step (determines the frequency range in harmonic analysis), and length of the simulations (important for having a sufficiently good frequency resolution). To model the short-circuited turns in FE simulations, the total ampere-turn of the affected pole is reduced accordingly. This means that the total ampere-turn of all poles is reduced. As a result, in the case of relatively severe faults, the terminal rms voltage is also noticeably reduced. This will be addressed later in this section. It should be noted that in practice, the output terminal voltage of the generator is kept constant and the effect of fault would be on the magnitude of the rotor field current, which will be
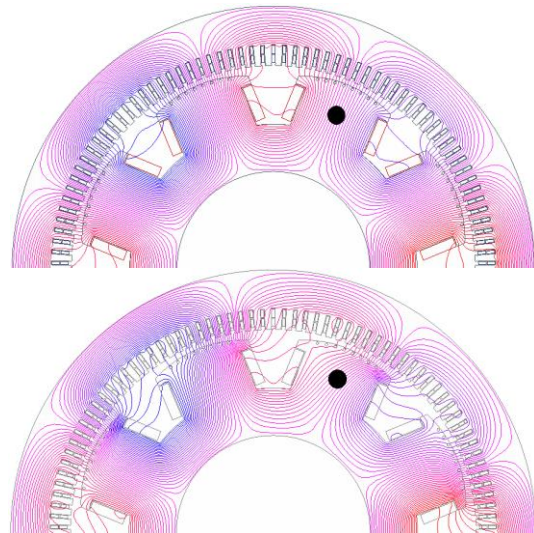

Fig. 1. Flux lines in no-load (top) and load (bottom) conditions in the case of 20 short-circuited turns (faulty pole is marked with a black circle).
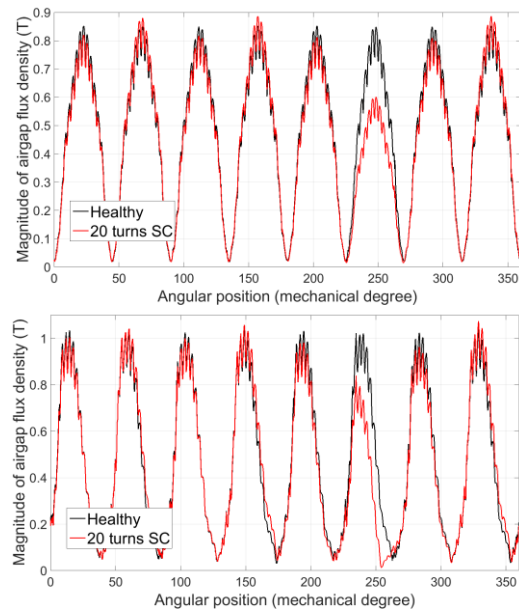

Fig. 2. Absolute value of airgap flux density in no-load (top) and load (bottom) conditions in the case of 20 short-circuited turns.

increased to compensate the reduction in the total rotor ampere-turn due to the short-circuited turns.

The hydropower generator, under study has 8 poles and 58 turns in each pole. In the simulations, the following six cases are included: healthy, 1 turn (1.7% of ampere-turn in the affected pole), 2 turns (3.4%), 5 turns (8.6%), 10 turns (17.2%), and 20 turns (34.5%) short-circuited. Both no-load and load conditions are considered in the study. Full-load operation is modeled using a coupled circuit where resistive loads (i.e. unity power factor) are connected to the terminals of the generator that are linked to the FE analysis. The generator is equipped with damper bars that are included in the FE analysis. Faulty cases are also modelled in an identical but damper-less generator in order to investigate the damper effects. The generator has no parallel circuits in the stator and all turns are

connected in series in each phase. In order to study the influence of parallel circuits, simulations are also carried out for an identical generator having two parallel circuits in the stator.

As mentioned before, the rms value of the induced terminal voltage of the generator is expected to reduce due to the fault. This is because the ampere-turn of the faulty pole and as a result the total ampere-turn of the rotor circuit is reduced. FE simulations show that the no-load induced terminal voltage is reduced by 0.21% (1 turn), 0.45% (2 turns), 1.1% (5 turns), 2.23% (10 turns), and 4.5% (20 turns) in the case of short-circuited turns. As predicted, inter-turn faults have a minor effect on the rms values of terminal voltage. The changes are almost negligible at the early stages of the fault. Hence, it is clear that reduction in the terminal voltage (in the simulations) or increase in the rotor field current (in practice) cannot be used for fault detection. Percentage of reduction in the terminal voltage is almost equal to the percentage of reduction in total ampere-turns of all poles. For instance, if 5 turns are short-circuited, the total rotor ampere-turn is $(7 \times 58 \times I_f + 1 \times 53 \times I_f)$, which is reduced by 1.1% compared to the total ampere-turn of a healthy generator, i.e. $8 \times 58 \times I_f$ (I_f is the rotor field current). Obviously, the higher the number of poles, the lower the overall effect of one faulty pole on the terminal voltage.

B. Analysis of Airgap Flux Density

Fig. 1 shows the flux lines in the generator with 20 short-circuited turns in one pole for both no-load and load conditions. It can be noticed that flux density is reduced in the faulty pole that is marked with a black circle. To better understand the effects of the fault on airgap field, flux density distribution in the airgap is plotted in Fig. 2 for both healthy and faulty (i.e. 20 turns short-circuited) cases and for both no-load and load conditions. As can be seen in the figures, the flux density in the faulty pole is significantly reduced. The amount of the reduction is similar to the reduction in total ampere-turns (34.5%) of the faulty pole. In addition to the pole having the sort-circuited turns, flux density distribution is affected in the other poles as well. The poles with the same polarity as the faulty pole experience a slight increase in the flux density, while the flux density is slightly reduced for the poles with the opposite polarity. This can be explained with the fact that the magnetic flux going outside of the rotor must be equal to the flux entering to the rotor. As a result, magnetic flux of all poles are somehow affected to compensate for the reduced ampere-turn in the faulty pole. This effect, also addressed in [3], is larger in the two adjacent poles as they share the flux with the faulty pole.

Spatial harmonics of radial flux density at no-load are shown in Fig. 3 for the healthy and faulty (20 turns short-circuited) cases. As seen in the figure, main component is the 4th harmonic, having the spatial order equal to the pole pair number (p). In addition, odd multiples of the main harmonics (i.e. 3rd, 5th, 7th, etc.) have a considerable amplitude. Two relatively high order harmonics (i.e. 122nd and 130th) produced due to the stator slots, having the spatial order equal to $N_s \pm p$, where N_s is the number of slots. As it is clear in Fig. 3 (bottom) in the case of inter-turn fault, many additional are created as a result
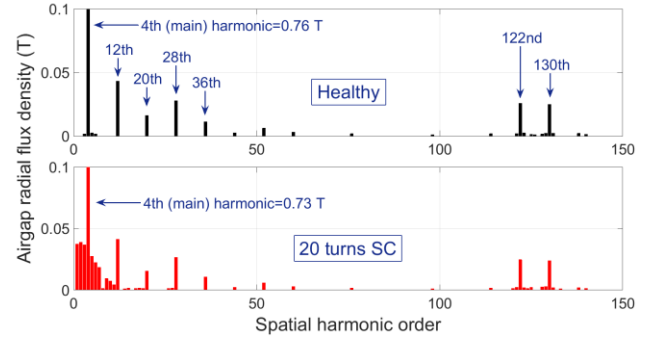

Fig. 3. Spatial harmonics of radial flux density at no-load for healthy and faulty (20 turns short-circuited) cases.
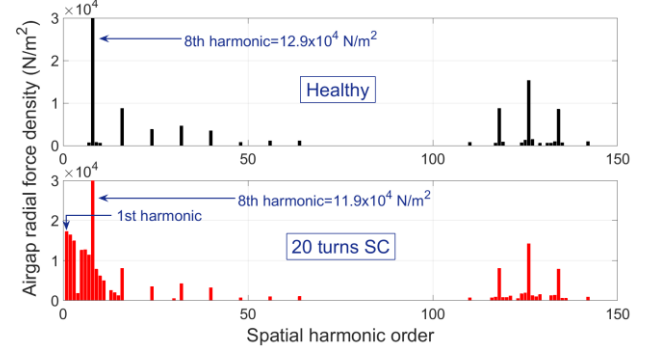

Fig. 4. Spatial harmonics of radial force density at no-load for healthy and faulty (20 turns short-circuited) cases.
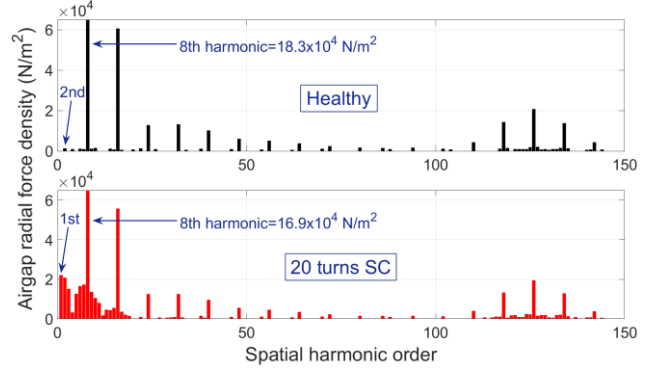

Fig. 5. Spatial harmonics of radial force density at full-load for healthy and faulty (20 turns short-circuited) cases.

of asymmetry in the flux density distribution. The major effect is indeed on low-order spatial harmonics, particularly sub-harmonics (i.e. 1st, 2nd, and 3rd). This is because, in the case of fault, there is no periodicity (i.e. identical repetition) anymore in the flux density distribution pattern.

C. Analysis of Radial Forces

Radial forces are among the main cause of vibration in electrical machines. Exciting radial electromagnetic forces are produced by interaction between different flux density harmonics and cause deformation in the stator. In this section, in order to study characteristics of radial forces, radial force density distribution is computed using Maxwell stress tensor:

$$f_r = \frac{1}{2\mu_0} (B_r^2 - B_t^2) \tag{1}$$

where B_r and B_t are radial and tangential components of flux

density in the airgap. From vibration perspective, the most important spatial in radial force density distribution are the ones with lowest orders. The reason is that the amplitude of stator deformations are inversely proportional to m^4, where m is the mode number (i.e. order of the spatial harmonic). For $m \geq 2$, the radial force distribution is symmetric in the airgap and there is no net force. For $m = 1$, the force distribution is not symmetric and the net force acting between the rotor and stator is not zero anymore. This is the case when eccentricity or inter-turn rotor faults exist, causing unbalance magnetic pull (UMP).

Fig. 4 and Fig. 5 shows the spatial harmonics of radial force density for no-load and load conditions, and for healthy and faulty (20 turns short-circuited) cases. As can be seen in the figures, 8th spatial harmonic is by far the largest component. Based on (1), this is the main force harmonic having the spatial order equal to $2p$ (i.e. pole number). However, this component is not critical form vibration perspective, due to a relatively high mode number. According to Fig. 4 (top), healthy generator does not have any low-order spatial force harmonics at no-load. As shown in Fig. 4 (bottom), inter-turn fault creates many additional spatial harmonics, particularly problematic low-order modes of vibration. Hence, the vibration level would significantly increase in the case a major fault. The most important consequence is the production of 1st harmonic ($m = 1$) and UMP. Radial force density distribution for a healthy generator at load, as shown in Fig. 5 (top), already includes a 2nd spatial harmonic ($m = 2$). This component is produced by the interaction between the main airgap field harmonic (4th) and MMF harmonics. Comparing Fig. 4 (top) and Fig. 5 (top), it can be concluded that the vibration level would notably increase when the generator is loaded, due to the presence of 2nd force harmonic. Similar to the no-load case, inter-turn fault would create additional low-order harmonics (including 1st order) and also significantly increase the amplitude of the 2nd spatial harmonic. Amplitude of the 1st radial force harmonic increases with the development of the fault and is equal to 1221 N/m², 6031 N/m², and 21880 N/m² when 1, 5, and 20 turns are short-circuited, respectively. The amplitude of the 2nd radial force is 1209 N/m² for the healthy generator and increases to 5725 N/m² and 21040 N/m² when 5 and 20 turns are short-circuited, respectively. As a result, major inter-turn faults would drastically increase the vibration level, due to UMP and other low-order force harmonics. Radial forces will be further discussed in Section IV and V, where effects of damper bars and parallel circuits are addressed (see Fig. 10 and Fig. 14).

III. FAULT DETECTION USING SPECTRAL ANALYSIS

In this section, electrical signature analysis is employed to detect rotor inter-turn faults. On-line detection method is based on spectral analysis of stator terminal voltage or current. Results presented here are based on the FE simulations of the original generator which is equipped with damper bars and has no parallel circuits. Sampling frequency and length of the signals used in spectral analysis are set to be 4 kHz and 1 second, in order to have a sufficiently good frequency resolution and range. Since FE model includes damper bars and
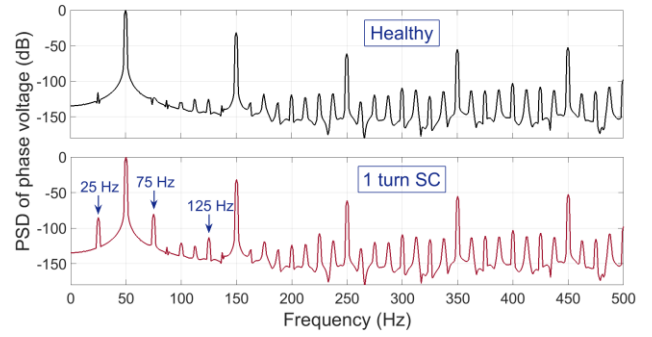

Fig. 6. Power spectral density of phase voltage at no-load for healthy and faulty (1 turns short-circuited) cases.
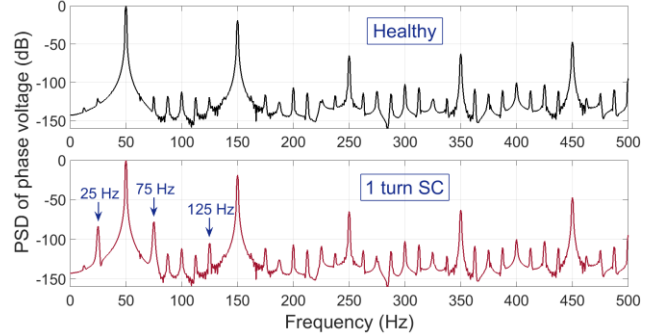

Fig. 7. Power spectral density of phase voltage at full-load for healthy and faulty (1 turns short-circuited) cases.
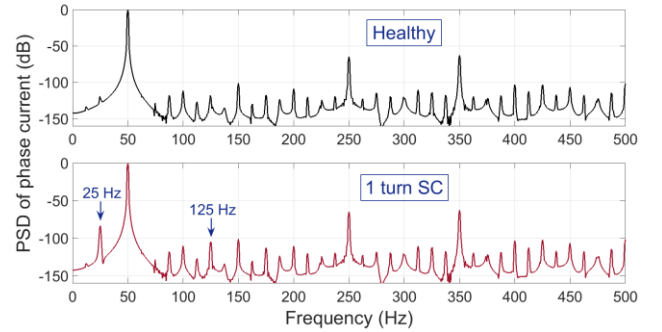

Fig. 8. Power spectral density of phase current at full-load for healthy and faulty (1 turns short-circuited) cases.

also parallel circuits (in some cases), the simulation length is set to be 2 seconds and the last 1 second of the simulated signals are used for spectral analysis. This is done to make sure that numerical transient period in the simulations does not affect the fault detection method. In the harmonic analysis, power spectral density (in dB) of signals are investigated, so the per unit amplitude of the fundamental 50 Hz component is 0 dB.

Fig. 6 and Fig. 7 show the PSD (power spectral density) of stator phase voltage in healthy and faulty (only one turn short-circuited) cases for both no-load and load conditions. As it is evident in both figures, well-known side band harmonics (at 25 Hz and 75 Hz) are drastically affected by the fault. Thus, the amplitude of these sideband harmonics can be used for fault detection at early stages. There are other fault-related harmonics in the spectrum, such as 125 Hz harmonic, as shown in the figures. In general, due to the asymmetry in the airgap flux density distribution, the fault would potentially induce the harmonics with the following frequencies in the stator voltage [7]:

TABLE II
AMPLITUDE OF FAULT-RELATED HARMONICS AT NO-LOAD (DECIBEL)

	25 Hz	75 Hz	125 Hz	225 Hz	1625 Hz	1725 Hz
Healthy	-112.3	-127.6	-125.1	-117.3	-103.8	-103.9
1 turn short-circuited	-85.25	-80.1	-112.9	-107.4	-94.2	-107.8
2 turns short-circuited	-79.1	-74	-107.9	-102.1	-88.9	-107.8
5 turns short-circuited	-71	-66	-100.4	-94.7	-81.4	-96.8
10 turns short-circuited	-64.9	-59.8	-94.6	-88.7	-75.1	-90.6
20 turns short-circuited	-58.6	-53.6	-88.6	-82.7	-68.8	-83.6

TABLE III
AMPLITUDE OF FAULT-RELATED HARMONICS AT FULL-LOAD (DECIBEL)

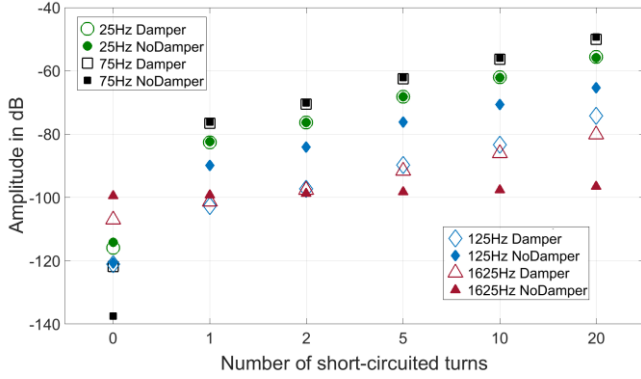|	25 Hz	75 Hz	125 Hz	225 Hz	1625 Hz	1725 Hz
Healthy	-115.9	-121.8	-121.1	-122	-107	-99.6
1 turn short-circuited	-82.6	-76.6	-102.7	-107.5	-101.4	-95.3
2 turns short-circuited	-76.3	-70.5	-97.3	-103	-97.6	-90.9
5 turns short-circuited	-68.2	-62.5	-89.8	-93.6	-91.6	-86.6
10 turns short-circuited	-62	-56.3	-83.3	-86.9	-86.1	-81.4
20 turns short-circuited	-55.6	-50	-74.2	-79.6	-80.1	-76

Fig. 9. Amplitude of fault-related harmonics at full-load in two cases: with and without damper bars.
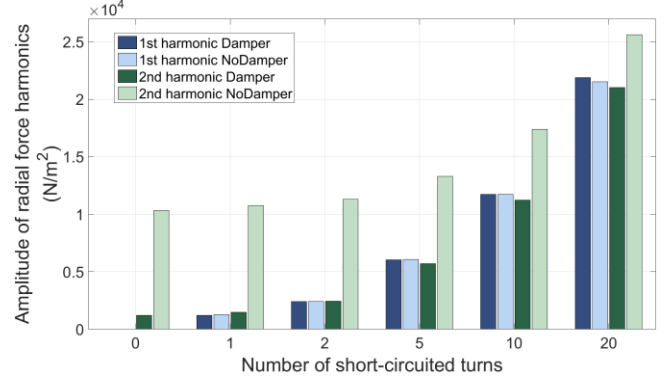

Fig. 10. Amplitude of radial force harmonics in in two cases: with and without damper bars.

$$f_{fault} = \left(1 \pm \frac{k}{p}\right) f_s \qquad (2)$$

where k is an integer and f_s is the fundamental frequency. As mentioned before, p is the number of pole pairs. In this regard, inter-turn faults in the rotor windings of salient pole machines are similar to demagnetization faults in permanent magnet synchronous machines. As discussed in [12], demagnetization fault would similarly give rise to the amplitude of the side band harmonics determined by (2).

Sideband harmonics adjacent to the fundamental component (i.e. 25 Hz and 75 Hz) corresponds to k=2 in (2) and there is no sideband harmonic with k equal to 1. Spectral analysis of stator voltage reveals that in addition to these sideband harmonics, a series of harmonics experience a continuous increase in the amplitude when inter-turn fault occurs and develops. These include but are not limited to harmonics at 100 Hz (k=4), 125 Hz (k=6), 225 Hz (k=14), 325 Hz (k=22), 375 Hz (k=26), 1625 Hz (k=126) and 1725 Hz (k=134). As can be seen, k is an even number for all the fault-related harmonics. Table II and Table III list the amplitude of selected harmonics in healthy and faulty

conditions. Even though amplitude of all listed harmonics increase with fault, it is evident that 25 Hz and 75 Hz harmonics are by far the most affected components and hence best candidate to be used as fault indices. According to the tables, the amplitude of the 25 Hz harmonic is increased by 27 dB (at no-load) and 33 dB (at full-load) when only one turn is short-circuited. Similarly, the amplitude of 75 Hz harmonic is increased by 47 dB (at no-load) and 45 dB (at full-load). These harmonics are most sensitive when fault occurs and then the rate of increase in the amplitude is reduced when fault develops. Base on the presented results, the amplitude of 25 Hz and 75 Hz harmonics can be used for detection of inter-turn faults at early stages. However, it is also important to monitor other fault-related harmonics, as they might help to distinguish between different types of fault.

In load conditions, a three-phase resistive load is connected to the terminals of the generator. Hence, it is expected to see the same pattern in the amplitude of the fault-related harmonics when spectral analysis of stator current is performed. The only exception is disappearance of certain harmonics, including fault-related ones, due to the connection of three phases. PSD

of stator phase current in healthy and faulty (one turn short-circuited) conditions is depicted in Fig. 8. As can be seen in the top figure, the 150 Hz (i.e. third harmonic of fundamental) component is drastically suppressed. This is because three phase windings are star-connected, without a grounded neutral and there is 3×120=360 degrees of phase shift between third harmonic currents of different phases. Due to the same reason, as can be seen in Fig. 8 (b), 75 Hz fault-related harmonic is disappeared. In this case, the phase shift between components from different phases is 1.5×120=180 degrees. Not having a grounded neutral means that this component is also canceled because of the winding connection. Similarly, 225 Hz and 1725 Hz harmonics are also disappeared in the PSD of phase current.

IV. EFFECT OF DAMPER BARS

The hydropower generator under investigation is equipped with damper bars. Hence, the original results in the previous sections are obtained using a FE model where dampers are activated. However, it is interesting to investigate the effect of damper bars on the proposed fault detection method. The motivation here comes from the potential contribution of dampers when airgap field includes additional spatial and temporal harmonics. For this purpose, all simulations are repeated for an identical generator, this time with removed damper bars.

Fig. 9 compares the amplitude of various fault-related harmonics of phase voltage in the loaded generator with and without damper bars. It is clear in the figure that the amplitude of two important fault-related harmonics (25 Hz and 75 Hz) are almost equal and they are not affected by dampers. However, damper bars affect the amplitude of two other harmonics in opposite ways. While rate of increase is slow down by dampers for 125 Hz harmonic, the changes in the amplitude of the 1625 Hz is only seen if dampers are activated. The most important conclusion is that damper bars does not affect the two important fault indices (25 Hz and 75 Hz) and hence their influence on the fault detection method can be considered insignificant. This could be due to the fact that the distorted flux density distribution (because of short-circuited turns) rotates synchronously with the rotor and dampers. Comparison between the healthy and faulty cases in the original generator reveals that damper eddy-current losses remain almost unchanged. This also confirms the insignificant effect of damper bars during the inter-turn faults.

In addition to the fault-related harmonics, the effects of damper bars on radial forces are also investigated. The amplitudes of 1st and 2nd radial force harmonics at full-load are shown in Fig. 10. According to the figure, the 1st harmonic (which produces UMP) is not affected by dampers. The reason may be that, as discussed in the previous paragraph, the distorted flux density spatial waveform rotates synchronously with the rotor. On the other hand, the amplitude of the 2nd radial force harmonic is significantly larger in the damper-less generator. For the healthy generator, the calculated value of 2nd harmonic is about eight times larger if dampers are removed. This is due to the fact that damper bars considerably reduce the
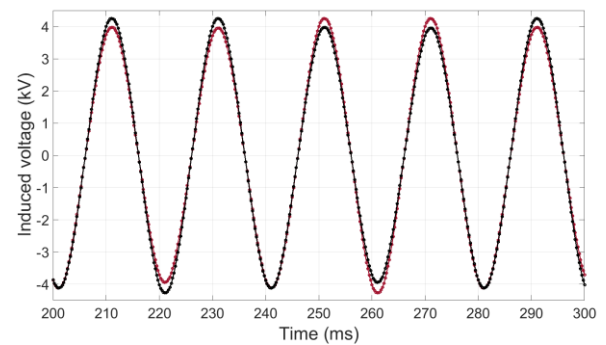

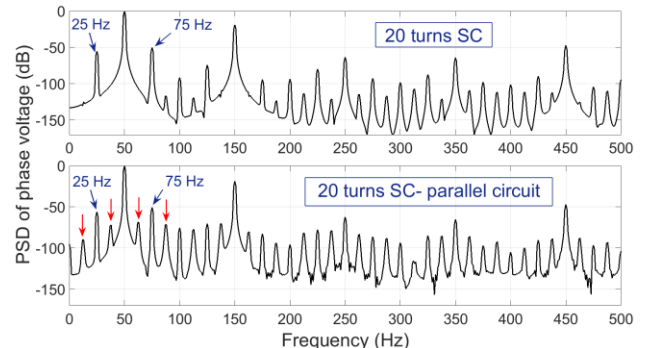Fig. 11. No-load induced voltage in two parallel windings.

Fig. 12. Power spectral density of phase voltage at full-load in the case of 20 short-circuited turns in two cases: with and without parallel circuits.
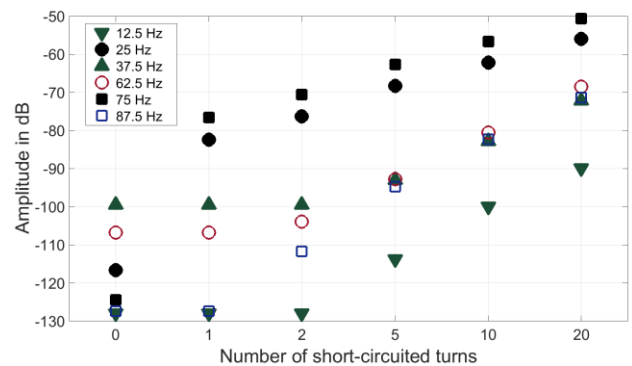

Fig. 13. Amplitude of fault-related harmonics at full-load in presence of parallel circuits in the stator windings.

amplitude of the sub- and inter-harmonics in the spatial distribution of airgap flux density. In healthy fractional-slot machines, the lowest order radial force (here is 2) is produced by the interaction between those harmonics and the main harmonic [10]. A reduction in the amplitude of the sub- and inter-harmonics in flux density due to the dampers would result in a reduction in the lowest radial force component and consequently vibration is reduced as well. Due to this reason, if the rotor of a hydrogenerator with fractional-slot windings is replaced with rotor of an induction machine (to enable variable-speed operation using doubly-fed induction machine), the vibration would considerably increase to unacceptable levels [14].

V. EFFECT OF STATOR PARALLEL CIRCUITS

It is not uncommon for large hydropower generators to be

equipped with two (most common) or more parallel circuits. In healthy conditions, the phase voltage induced in two parallel windings is equal. However, in the case of magnetic unbalance (including inter-turn rotor fault) the induced voltage is not equal anymore causing a circulating current. Measurement of this circulating current could be used as a fault detection technique. In presence of parallel circuits, there will be a counter filed produced by the circulating current, opposing the field which has induced the current. Due to this contribution, it is reported that UMP caused by magnetic unbalance (due to eccentricity or inter-turn faults) is considerably lower in the case of parallel circuits [3].

Due to the important contribution from the parallel circuits in the case of magnetic unbalance, it is necessary to investigate the performance of the proposed fault detection method in presence of parallel circuits. For this purpose, a new FE model of the generator, this time equipped with two parallel circuits, is built and simulated because the original generator does not have any parallel circuits. In the case of parallel circuits, the total phase voltage is halved and the total phase current is doubled. It is important to note that the current loading (i.e. current density in the stator slots) remains unchanged. Fig. 11 shows the no-load induced voltage in the two parallel windings. As can be seen in the figure, the induced voltages are different and as a result, a circulating current is produced when the generator is loaded.

Fig. 12 compares the PSD of phase voltage for case with and without parallel circuits when 20 turns are short-circuited. The amplitude of the main fault indices (i.e. 25 Hz and 75 Hz harmonics) remain unchanged. However, as it is clear in the figure, new fault-related harmonics appear in the frequency spectrum. In the frequency range below 100 Hz, four new harmonics (marked with red arrows) are 12.5 Hz, 37.5 Hz, 62.5 Hz, and 87.5 Hz. Based on (2) these harmonic are produced with values of k equal to 1 and 3. In the original generator, fault-related harmonics have the even values of k, while in presence of parallel circuits, new harmonics are generated having k equal to odd numbers. However, these new harmonics are not produced in the case of minor faults and appear when the faults develop. Fig. 13 shows how the amplitude of 12.5 Hz, 37.5 Hz, 62.5 Hz, and 87.5 Hz harmonics changes with fault severity. According to the figure, the amplitude of these harmonics considerably increase when 5 or more turns are short-circuited. This is in contrast with 25 Hz and 75 Hz harmonics (also shown in the figure) which are most sensitive to the minor faults. Here, the important conclusion is that the proposed method can be effectively used in the case of parallel circuits as well and the amplitude of the main fault related harmonics remain unchanged compared with the original generator.

Fig. 14 shows the effect of parallel stator windings on the amplitude of radial force harmonics. As expected, in presence of parallel circuits, the amplitude of 1st radial force harmonic is considerably reduced (more than 50%). Consequently, as discussed before, UMP can be reduced if the stator is equipped with parallel circuits. On the other hand, the amplitude of the 2nd radial force harmonic is almost unchanged. This is because the spatial flux density harmonics which produce the second
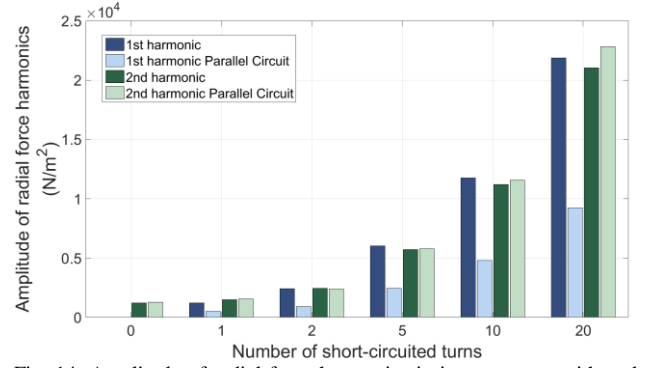

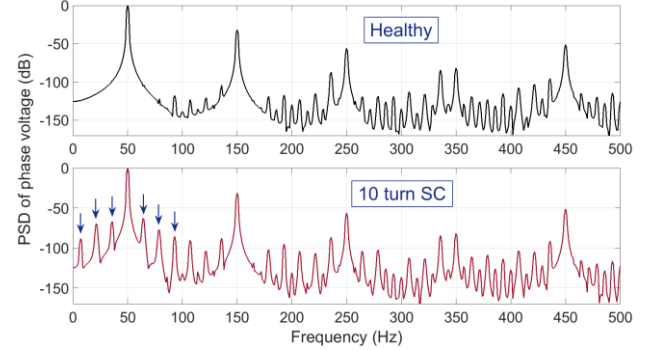Fig. 14. Amplitude of radial force harmonics in in two cases: with and without parallel circuits.

Fig. 15. Power spectral density of phase voltage at no-load for healthy and faulty (10 turns short-circuited) cases in a 14-ploe generator.
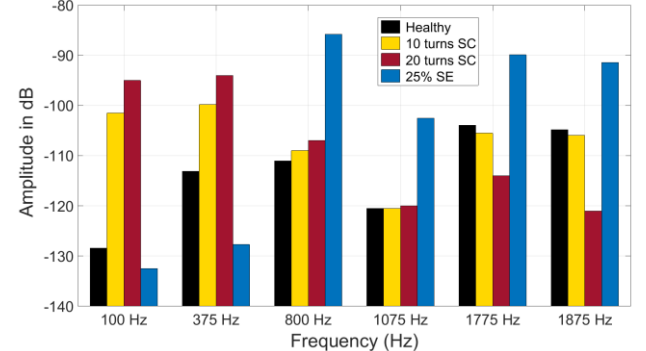

Fig. 16. Amplitude of fault-related harmonics at no-load in the case of eccentricity and rotor inter-turn faults.

mode of vibration are not affected by parallel circuits in the stator windings.

VI. INFLUENCE OF POLE PAIR NUMBER

According to (2), the frequency of fault-related depends on the pole pair number. To see the effect of pole pair number, another hydropower generator with 14 poles is modeled and simulated using FE analysis. Fig. 15 shows the PSD of no-load phase voltage in this generator when 10 turns out of 50 turns in one rotor pole are short-circuited. As can be seen in the figure, new harmonics appear in the case of fault, including 7.1 Hz, 21.4 Hz, 35.7 Hz, 64.3 Hz, 78.6 Hz and 92.9 Hz (marked with blue arrows). These frequency of this harmonics can be calculated based on (2), with k equal to 2, 4, and 6. Similar to the original 14-pole generator, k is equal to an even number for the fault-related harmonics.

VII. Comparison with Eccentricity Fault

In this section, a comparison between PSD of no-load phase voltage in the case of rotor inter-turn and dynamic eccentricity faults is presented. The reason is that eccentricity can create the same fault-related harmonics and this can make it difficult to identify the type of fault. It is not within the scope of this paper to distinguish between eccentricity and inter-turn faults, as it needs more comprehensive analysis. This section aims to highlight which harmonics are more affected by eccentricity than inter-turn fault and vice versa. For this purpose, the original generator is modelled with 25% dynamic eccentricity (SE) and the results are compared with the case of inter-turn faults.

As expected, results show that amplitude of some harmonics (including important 25 Hz, 75 Hz and 125 Hz harmonics) increases with both inter-turn and eccentricity faults. However, as depicted in Fig. 16, there are a couple of harmonics which are only affected by inter-turn fault (i.e. 100 Hz and 375 Hz) and not dynamic eccentricity. On the other hand, there exists a series of harmonics which are considerably more affected by eccentricity fault (i.e. 800 Hz, 1075 Hz, 1775 Hz and 1875 Hz). This shows that it might be possible to distinguish between these two types of faults using the spectral analysis of phase voltage or current and monitoring a series of fault-related harmonics. However, no conclusion can be made here, since it requires a comprehensive investigation of static and dynamic eccentricity cases. As mentioned before, this is beyond the scope of this paper.

VIII. Conclusion

In this paper, inter-turn faults in the rotor of salient-pole synchronous machines are investigated using FE analysis. The machine under study is a 22 MVA 8-pole hydrogenerator. Presented electromagnetic analysis includes investigation of flux density and radial force density distributions in the airgap. It is shown that spectral analysis of stator voltage or current can be used to detect the rotor inter-turn faults in early stages. Fault-related harmonics are introduced and it is shown that their amplitudes increase when the fault develops. It is shown that damper bars do not affect the main fault-related harmonics and UMP. However, they significantly reduce the amplitude of the 2nd radial force harmonic. In addition to the original generator, the effectiveness of the proposed fault detection method is confirmed when stator is equipped with parallel circuits. In this case, it is revealed that while amplitude of the main fault-related harmonics remains unchanged, new harmonics appear in the voltage PSD. It is also shown that UMP is considerably reduced because of parallel circuits while amplitude of the 2nd radial force harmonic is unchanged. In order to highlight the influence of pole pair number, another generator with 14 poles is simulated in healthy and faulty conditions. In addition, a comparison between PSD of no-load induced voltage in the case of dynamic eccentricity and rotor inter-turn faults is presented. It is revealed that while some fault-related harmonics (including main fault indices) are similarly affected by both types of faults, there exists a number of harmonics which are only affected by one of them.

References

[1] P. Tavner, L. Ran, J. Penman, H. Sedding, *Condition monitoring of rotating electrical machines*, IET Power and Energy Series 56, 2008.
[2] G. C. Stone, M. Sasic, J. Stein, C. Stinson, "Using magnetic flux monitoring to detect synchronous machine rotor winding shorts," in *Proc. IEEE PCIC*, 2011, pp. 1-7.
[3] M. Wallin, U. Lundin, "Dynamic unbalanced pull from field winding turn short circuits in hydropower generators," *Electric Power Components and Systems (Taylor & Francis)*, vol. 41, pp. 1672-1685, 2013.
[4] B. M. Babic, S. D. Milic, A. Z. Rakic, "Fault detection algorithm used in a magnetic monitoring system of the hydrogenerator," *IET Electric Power Applications*, vol. 11, no. 1, pp. 63-71, 2017.
[5] W. Shuting, L. Heming, L. Yonggang, M. Fanchao, "Analysis of stator winding parallel-connected branches circulating current and its application in generator fault diagnosis," in *Proc. IEEE IAS Annual Meeting*, 2005, pp. 42-45.
[6] M. Cuevas, R. Romary, J. Lecointe, T. Jacq, "Non-invasive detection of rotor short-circuit fault in synchronous machines by analysis of stray magnetic field and frame vibrations," *IEEE Tran. Magnetics*, vol. 52, no. 7, July 2016, Art. no. 8105304.
[7] H. Toliyat, S. Nandi, S. Choi, H. Meshgin-kelk, *Electrical machines: modeling, condition monitoring, and fault diagnosis*, CRC Press, 2013.
[8] H. Henao *et al.*, "Trends in fault diagnosis for electrical machines: a review of diagnostic techniques," *IEEE Industrial Electronics Magazine*, vol. 8, no. 2, pp. 31-42, 2014.
[9] J. Faiz, B. M. Ebrahimi, B. Akin, H. A. Toliyat, "Comprehensive eccentricity fault diagnosis in induction motors using finite element method," *IEEE Tran. Magnetics*, vol. 45, no. 3, pp. 1764-1767, March 2009.
[10] A. Mahyob, P. Reghem, G. Barakat, "Permeance Network Modeling of the stator winding faults in electrical machines," *IEEE Tran. Magnetics*, vol. 45, no. 3, pp. 1820-1823, March 2009.
[11] C. P. Salomon *et al.*, "Discrimination of synchronous machines rotor faults in electrical signature analysis based on symmetrical components," *IEEE Tran. Industry Applications*, vol. 53, no. 3, pp. 3146-3155, May/June 2017.
[12] M. Zafarani, T. Goktas, B. Akin, "A comprehensive magnet defect fault analysis of permanent-magnet synchronous motors," *IEEE Tran. Industry Applications*, vol. 52, no. 2, pp. 1331-1339, March/April 2016.
[13] E. L. Engevik, M. Valavi, A. Nysveen, "Influence of winding layout and airgap length on radial forces in large synchronous hydrogenerator," in *Proc. ICEMS*, 2017.
[14] T. Lugand, A. Schwery, "Comparison between the salient-pole synchronous machine and the double-fed induction machine with regards to electromagnetic parasitic forces and stator vibrations," *IEEE Tran. Industry Applications*, Early Access.

Mostafa Valavi received his PhD degree in 2015 from the Norwegian University of Science and Technology (NTNU), Trondheim, Norway. Since then, he has been a postdoctoral research fellow at NTNU.

Kari Gjerde Jørstad received her M.Sc. degree from Norwegian University of Science and Technology (NTNU) in 2017. She is now with Norconsult.

Arne Nysveen received his Dr.ing. in 1994 from Norwegian Institute of Technology (NTH). From 1995 to 2002 Nysveen worked as a research scientist at ABB Corporate Research in Oslo, Norway. Since 2002 Nysveen has been a professor at the Norwegian University of Science and Technology (NTNU). He is the Work Package Manager for turbine and generator technologies in Norwegian Research Centre for Hydropower Technology (HydroCen).